Fabrication and characterization of ZnO/Ag nanocomposite using *phoenix dactylifera* mucilage for antibacterial applications

A. Iqbal [a], M. F. Ijaz [b*], M. A. Dilbraiz [c], T. Tahir [d], I. Ahmed [e], Y. Iqbal [a, f,*], K. Shahzad [g]

[a] *Department of Chemistry, University of Sialkot, Sialkot 51040, Pakistan*
[b] *Department of Mechanical Engineering, College of Engineering, King Saud University P.O. Box 800, Riyadh, 12372, Saudi Arabia*
[c] *Department of Applied Sciences, Pakistan Navy Engineering College NUST Karachi, Pakistan*
[d] *Department of Nuclear Research, Center for Physical Sciences and Technology, Savanorių Ave. 231, LT-02300 Vilnius, Lithuania*
[e] *Department of Industrial Engineering, University of Rome Tor Vergata, Rome 00133, Italy*
[f] *Department of Chemistry, Baba Guru Nanak University, Nankana Sahib-39100, Pakistan*
[g] *Department of Physics, Baba Guru Nanak University, Nankana Sahib-39100, Pakistan*

The central focus of this work was to synthesize a ZnO/Ag nanocomposite employing a sustainable, cost-effective, and eco-friendly approach with fewer harmful chemicals. The mucilage of the date palm (*Phoenix dactylifera*) was utilized for the purpose of capping and sealing. The synthesized ZnO/Ag exhibited a face-centered cubic structure of Ag and a hexagonal wurtzite crystalline phase. Their mean crystallite size was 25 nm. Scanning electron microscopy revealed that the particles have a spherical morphology. The antibacterial efficacy of the fabricated ZnO/Ag nanocomposite was evaluated against the bacterial strains *S. aureus, B. subtilis, E. coli, A. hydrophila*, and *B. cereus* using the agar well diffusion technique. The ZnO/Ag nanocomposite generated inhibitory zones of 15.3 ± 0.58 mm, 15.7 ± 0.58 mm, 15.5 ± 0.5 mm, 11.4 ± 0.51 mm, and 10.6 ± 0.58 mm, respectively. In the future, antibacterial biobased bandages for wound healing and hand sanitizers may be developed utilizing the ZnO/Ag nanocomposite, which has demonstrated antibacterial efficacy and was produced by a cost-effective and eco-friendly method.

(Received May 9, 2025; Accepted August 20, 2025)

Keywords: Nanohybrid, Date palm mucilage, Antibacterial, ZnO/Ag, XRD, SEM

1. Introduction

The rise of antibiotic resistance has paved the way to ongoing research into the development of versatile antibiotic agents. Currently nano-materials because of their better surface area to volume ratio and some other peculiar properties have got attention in this regard [1]. There has been a boom in nanotechnology research in the 21st century. It includes the study of the fabrication of new structures, using different techniques and tools, with particle size less than 100 nm [2]. The multidisciplinary study of nanomaterials due to versatile applications is evidence of the importance of nanotechnology [2, 3]. Control on size growth opens door for tuning certain peculiar properties of the material because it became facile to modify phase stability and electronic makeup of the material [4-6]. Bio-nanotechnology is an emerging field at the interface of biotechnology and nanotechnology. It focuses on synthesis of nanomaterials through biosynthetic approaches [7]. Metal nanoparticles have been reported as efficacious agents in different fields like catalysis and biological studies. Among the other metals such as Zn, Cu, Ti, Mg, and Au, the Ag nanoparticles have been

* Corresponding authors: mijaz@ksu.edu.sa
https://doi.org/10.15251/JOBM.2025.173.173

proven more effective against microorganisms such as fungus, viruses, and bacteria [8, 9]. It has also been used in chronic wounds and burn treatment [10, 11]. Silver nitrate has also been reported for removal of granulation tissues as it accelerates crust formation on wound surface and allows epithelization [12, 13]. Use of Ag as antimicrobial was decreased after discovery of penicillin [14]. In recent time it again emerged when Moyer reported 0.5% AgNO3 solution non-interference with epidermal proliferation along with possessing the antibacterial properties against *E. coli, P. aeruginosa,* and *S. aureus* [15, 16].

However, Ag nanoparticles pose some side effects such as Argyria, Argyrosis and toxicity to mammalian cell [17, 18]. But the ongoing investigation endorses the fact that either metallic or silver ion can be a potent agent in burn treatment, stainless steel materials, dental materials, sunscreen lotions, water treatment. It can be mended in a way to pose less toxicity against cells of humans with reduced volatility and enhanced thermal resistance [19]. One of the ways to enhance Ag efficacy is fabrication of its composites. A hybrid of two or more metals or metal oxides resulting in formation of new material with unique physiochemical properties is the trend of current research that has different applications [20]. Synthesis of inorganic antimicrobial agents is the recent research area to control the growth of microbes. Inorganic antimicrobial agents have long shelf life and are more stable at high temperature and pressure as compared to organic antimicrobial [21]. Among nanocomposites, ZnO/Ag has attained attention because ZnO is less toxic, chemically stable and has great antibacterial effect on both gram (+) and gram (-) bacteria [22]. Ag NPs have both antibacterial and antifungal effects. ZnO NPs show antimicrobial activity by disrupting the integrity of cell membrane. This increase permeability through cell membrane that led to accumulation in the cytoplasm and ultimately disruption of cell [23, 24]. As ZnO is bactericidal, the deposition of silver metal can improve the antibacterial activity of ZnO [25]. The other retarding factor is the synthesis method. As the world is much concerned about the environment now a days and green chemistry is getting attention for the sake of this. To date, different physiochemical methods have been used to synthesize various materials. Expensive solvents, harmful reagents and specific instrumentation are required to synthesize these. Green synthesis is an alternative approach to avoid all these obstacles. Green synthesis is easy to handle, cost effective, best for large scale production, economical and energy efficient [25]. Synthesizing using the green synthesis approach results in NPs with homogeneous chemical composition, perfect surface structure and minimum defects [26]. Synthesis of nanoparticles by using renewable plant sources are of significant interest in the biomedical field. These are biologically compatible and non-toxic. Regarding the finest of our times, there is no study for the formation of ZnO/Ag nanocomposite by using date palm mucilage (DPM) as a plant source.

In the present work ZnO/Ag nanocomposite is fabricated by using DPM as reducing and capping agent with precursor salts of zinc nitrate hexahydrate and silver nitrate [27]. A large number of excipients obtained from plants are available in the form of starch, chitosan, sugar, gelatin, gum, cellulose, pectin and mucilage. These excipients swell up when they are exposed to water. Plants that have normal growth give mucilage as a metabolite within the plant cells. Mucilages are partially soluble in water and give greasy stuff. Up to 88.01 % carbohydrates are present in mucilage. Mucilage also contains sugar which act as reducing agent. DPM produces no toxicity towards human health [28]. This investigation has focused on adding the synergistic antibacterial properties of ZnO nanoparticles and silver nanoparticles through the development of a ZnO/Ag nanocomposite. Open wounds result from the loss of skin and subcutaneous tissues. It induces external hemorrhaging. It can cause spread of germs into deeper layers and lymph nodes. Proper wound coating is needed to control the growth of pathogens at wounds. Betadine is an excellent antimicrobial solution to kill all type of pathogenic microorganisms, but it can also cause renal failure, allergic reactions and some other abnormalities in some patients. Similarly, alcohol can also cause irritation and destroy cells. *Pseudomonas aeruginosa* and *Acinetobacter baumannii* bacteria cause infection in burn wound. It develops resistance against common antibacterial agents. Therefore, it is needful to synthesize new antimicrobial agents [29]. To deal with drug resistant microbes, in current research ZnO/Ag nanocomposite is fabricated by eco-friendly method.

2. Experimental

2.1. Materials

Every chemical reagent used in the investigation was analytical grade. The chemicals were purchased from a registered company (Asia Scientific, Faisalabad, Pakistan). The chemicals and reagents used for the synthesis of ZnO/Ag nanocomposite were silver nitrate, zinc nitrate hexahydrate, NaOH, ethanol and deionized water. Date palm mucilage was purchased from an herbal medicinal store located in Faisalabad.

2.2. Pretreatment of date palm mucilage

DPM (*Phoenix dactylifera*) was used as the target sample as shown in Fig. 1. for the green synthesis of ZnO/Ag nanocomposite. It was purchased from herbal medical store sited in Sialkot, Pakistan. The polythene was removed from the raw sample of DPM and then ran many times using pure water. Following the dissolution of DPM in water, the mix was agitated for an hour at room temperature and then filtered through a nankeen cloth to remove any solid contaminants [23, 28].

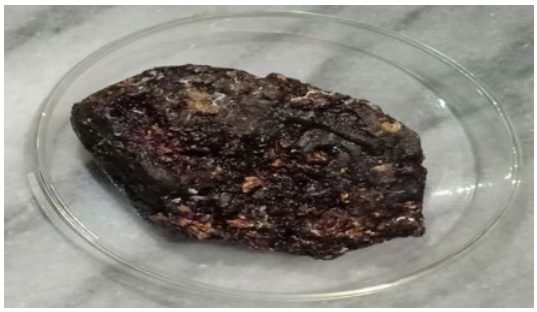

Fig. 1. Date palm mucilage (Phoenix dactylifera).

2.3. Biosynthesis of ZnO/Ag nanocomposite

ZnO/Ag nanocomposite was synthesized by dissolving $AgNO_3$ (0.1M 50 ml) solution in $ZnNO_3.6H_2O$ (0.5M 50 ml) solution using method [30] with modification. Schematic representation of biosynthesis of ZnO/Ag nanohybrid is shown in Fig 2. The resultant solution was stirred for 2 min leading to appearance of white color. Then NaOH (1M) solution was added dropwise that resulted in the formation of light-yellow precipitates. After that, the extract of DPM was added into the above solutions that changed into light brown color. The sample was then placed in hot air oven at 100 °C for 6 h and the sample changed its color from light brown to dirty brown. The sample was allowed to cool at room temperature. The acquired sample underwent two washes with distilled water and two washes with ethanol; each performed at 6000 rpm for a duration of 10 minutes. The final product was subjected to drying at 60 °C in a hot air oven followed by calcination at 350 °C for five hours.

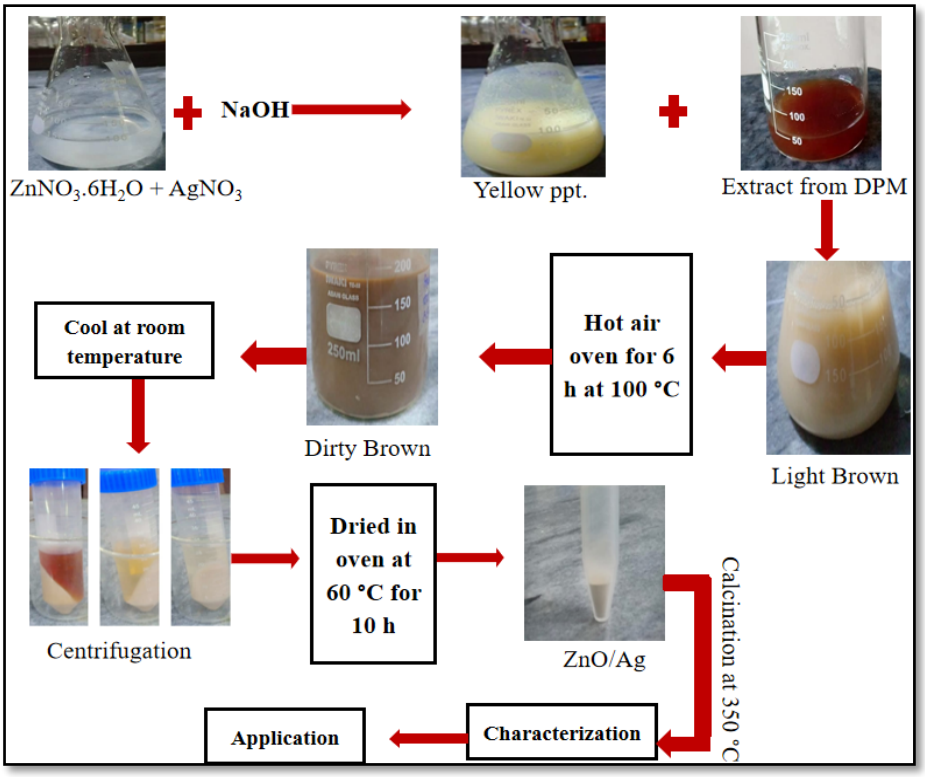

Fig. 2. Schematic representation of biosynthesis of ZnO/Ag nanohybrid.

2.4. Characterization of synthesized ZnO/Ag nanocomposite

ZnO/Ag nanocomposite was characterized using X-ray Diffraction (XRD) (D8 Bruker system). The acquired XRD pattern was compared with the Joint Committee on Powder Diffraction Standards (JCPDS) file. The Malvern Zetasizer 2000 was utilized to determine the average particle size of ZnO/Ag nanohybrid. Water, being non-interfering, having viscosity of 0.8872 cP and refractive index of 1.3 was used as dispersant solvent. The set preferred solution temperature was 25 °C and clear disposable zeta cell were utilized as specimen holder. The sample was exposed to the beam of laser that scattered light in different intensities. The scattered light was detected with count rates of 166.3 kcps. The surface morphology of ZnO/Ag nanocomposite was analyzed by scanning electron microscope (JSM5910, JEOL, Japan) at various scales and magnification powers. The images were taken at different magnifications. The accelerating voltage of 10 kV was used for SEM images.

2.5. Antibacterial evaluation

The agar disc diffusion method was employed to assess antibacterial activity. The evaluation of antibacterial activity utilized strains of *S. aureus*, *B. subtilis*, *E. coli*, *A. hydrophila*, and *B. cereus*. Ciprofloxacin for (*S. aureus*, *B. Subtilis*) whereas gentamicin for (*E. coli*, *A. hydrophila* and *B. cereus*) were used as control. The nutrient agar (28 g/1000 L) was autoclaved for 15 minutes at 121 °C. The inoculation of bacterial strains was taken place on nutrient agar. The nutrient agar was shifted to petri plates. The sterile cork was employed to create an aperture measuring 6mm and disks containing samples and standards were placed on the holes. 40 mg/ml of test agent (ZnO/Ag nanocomposite) were prepared and 100 µL solution loaded into disk. The agar plates underwent incubation for a duration of 24 hours. Clear zones appeared in sample wells that showed inhibition of bacterial growth. The zone reader was applied to measure zone of inhibition by keeping ciprofloxacin and gentamicin as standard [23].

2.6. Statistical analysis

The data obtained was computed and analyzed by MS Excel. The data was statistically analyzed by mean ± standard deviation. The results were displayed in the form of mean and standard deviation range.

3. Results and discussion

The purpose of the current work was to investigate the antibacterial activity of the ZnO/Ag in light of claims that were made in earlier researches. This work used palm mucilage (Phoenix dactylifera) as a capping and reducing agent to produce a ZnO/Ag nanocomposite via a green process. The mucilage used in the study was extracted from the date palm's dried fruit. It comes in pellet shape and has a dark brown hue. It is readily accessible in Pakistani herbal medicine stores and is a mainly composed of carbohydrates. The mucilage is reducing in nature, has ability to bind, has high viscosity, and solubility in water [31].

3.1. X-ray diffraction analysis (XRD)

The (XRD) analysis of the ZnO/Ag nanocomposite was performed to investigate its crystalline makeup, phase design, and crystallite size. The data was gathered in the 2θ range of 0°–70° that revealed characteristic peaks corresponding to the hexagonal wurtzite structure of ZnO and the cubic face-centered (fcc) structure of metallic silver (Ag). The observed ZnO peaks at as 31.5°, 34.5°, 36.2°, 47.6°, 63°, 68° and 69° were indexed to planes such (100), (002), (101), (102), (112), (200) and (201) respectively. The respective peaks matched with standard JCPDS of ZnO (36-1451). The Ag peaks at 38° and 66.3° were identified at positions corresponding to planes (111) and (103) exhibited face-centered cubic structure of Ag. The data was matched with the JCPDS of Ag (04-0783) that confirms the presence of metallic silver.

The XRD data was refined using the Rietveld refinement method implemented in the FullProf software. Initial structural models for ZnO and Ag were input, and the refinement process optimized several parameters, including lattice constants, atomic positions, crystallite size, microstrain, and phase composition. The refinement quality was evaluated using statistical fit chi square $\chi 2$, with a good fit indicated by $\chi 2 \approx 2.63$and low RRR-factors. The refined lattice parameters for ZnO were $a \approx 3.25$ A˚ and $c \approx 5.20$ A˚, closely matching the values reported for bulk ZnO. For the Ag phase, the refined lattice parameter was $a \approx 4.08$ A˚, consistent with the cubic fcc structure. The average crystallite size of the ZnO phase, calculated by using Deby Scherer's equation from broadening peaks and found to be 25 nm, while the Ag crystallite size was estimated to be 20 nm. Micro strain effects were minimal, indicating good crystallinity of the synthesized nanohybrid. The phase composition analysis revealed that ZnO constituted approximately 85–95 wt%, while Ag contributed 05–15 wt%. A slight preferred orientation was observed for the ZnO phase along the (002) plane, reflecting anisotropic growth behavior typical of ZnO nanostructures.

The ZnO/Ag nanohybrid's successful fabrication was verified by the XRD analysis, with no significant lattice distortions observed in the ZnO phase due to Ag incorporation. The refined structural parameters and phase composition highlight the nanoscale nature and quality of the hybrid material). No diffraction peak was found for any impurity. Moreover, the intensity of Ag peak was lower than the intensity of ZnO peak. It anticipated the low percentage of Ag in ZnO/Ag nanohybrid. Additionally, the results are consistent with the results that were reported by [32]. Ag and ZnO started to show definite, separate phases in ZnO/Ag nanocomposite corroborate the synthesis of target nanohybrid. The presence of Ag nanoparticles is expected to enhance the functional properties of ZnO, such as photocatalytic activity and antibacterial efficacy, through plasmonic interactions.

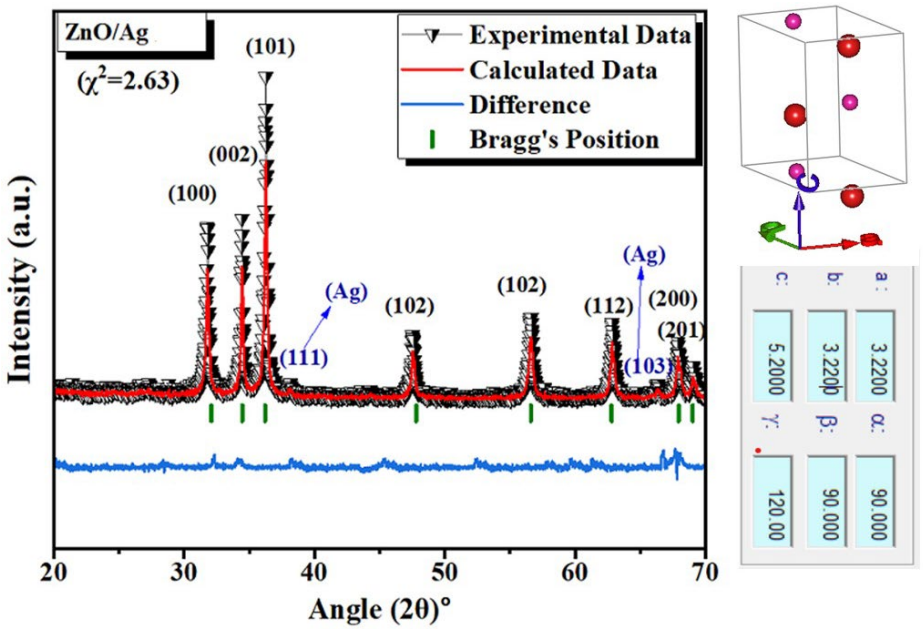

Fig. 3. X-ray diffraction pattern of ZnO/Ag nanocomposite, refinement was carried out using full proof suit software and parameters were calculated using software.

3.2. DLS analysis

The stability of ZnO/Ag and particle size dispersion was analyzed by dynamic light scattering and results are outlined in Fig. 4 (a, b). The sample was exposed to laser beam and the pattern of scattering of light with different intensities was obtained. The size of the particles was determined by DLS measuring Brownian motion of particles in solution and using that motion as guide. As compared to larger particles, smaller particles scattered quickly due to the fast change in light scattering intensity. The Stokes-Einstein equation was utilized to ascertain the particle size distribution through the application of the diffusion coefficient. The determined particle size of ZnO/Ag was 201.7 nm with 94.3 nm corresponding to peak 1 and another peak 2 appeared at 4373 nm with 5.7% intensity that may be due to presence of mucilage material along with nanohybrid (Fig. 4b). The polydispersity index of ZnO/Ag nanocomposite was 0.258 with average particle size of 183.4 nm. Fig.4a clearly showed single distinct peak of zeta potential at 7.57 mV with 100% intensity. The measurement of zeta potential was taken to ascertain the surface charge of the nanohybrid within the colloidal solution. There was a charge on ZnO nanoparticles surface that attracted the counter ion of Ag nanoparticles surface. It resulted in forming a double layer of counter ions that induced electric potential which is known as zeta potential of nanohybrid. The surface charge of nanomaterials is linked to the efficiency of product, particles with zeta potential in range of +30 mV and -30 mV have stability and effectiveness [32]. The smaller value of zeta potential indicated that attraction existed between nanoparticles (ZnO & Ag) of nanocomposite (ZnO/Ag). The particles have potential stability. The size of nanoparticle can be controlled by changing the concentration of plant extract, as discussed by Kharissova et al [33].

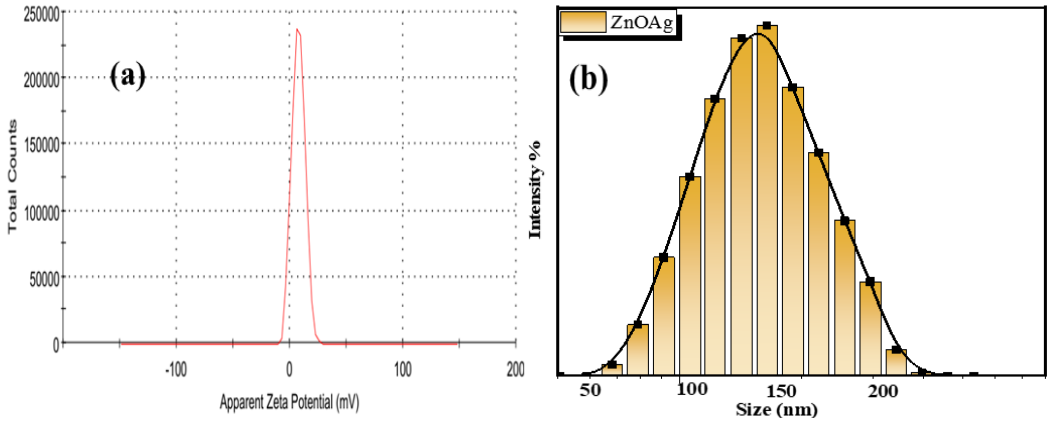

Fig. 4. a) Zeta potential of ZnO/Ag nanohybrid. b) Size distribution graph of ZnO/Ag nanohybrid.

3.3. Surface morphological analysis

Scanning Electron Microscopy (SEM) was employed to examine the outermost morphological concepts of the synthesized ZnO/Ag nanocomposite. SEM produced images of ZnO/Ag by scanning its surface by a beam of electrons. Electrons interacted with atoms of sample that produced different signals. These signals gave information about the topography of ZnO/Ag nanohybrid. The position of beams was combined with intensity of detected signals that produced an image of sample. The secondary electron detector was used to detect the number of secondary electrons emitted by atoms. The surface of sample was scanned via different magnification powers ranging from 4 kx to 200 kx and scales from 10 µm to 200 nm. It gave 3D black and white image of ZnO/Ag nanocomposite (Fig. 5). The maximum resolution was achieved at the magnification power of 200000 with scale 200 nm (Fig. 5g). The particles were found to be spherical. The particles of bigger size might be ZnO that might be surrounded by some smaller particles of silver via electrostatic interactions. The particles were arranged in a consistent manner. Reported that the structure of ZnO was covered by non-uniform distribution of Ag with 40.51 µm thickness. ZnO nanomaterials showed structured clusters with average diameter of 40-50 nm and the Ag material possessed hexagonal solid structure with average diameter of 150-200 nm as reported in literature [34]. It was found that ZnO material was surrounded by silver material with smooth surface.

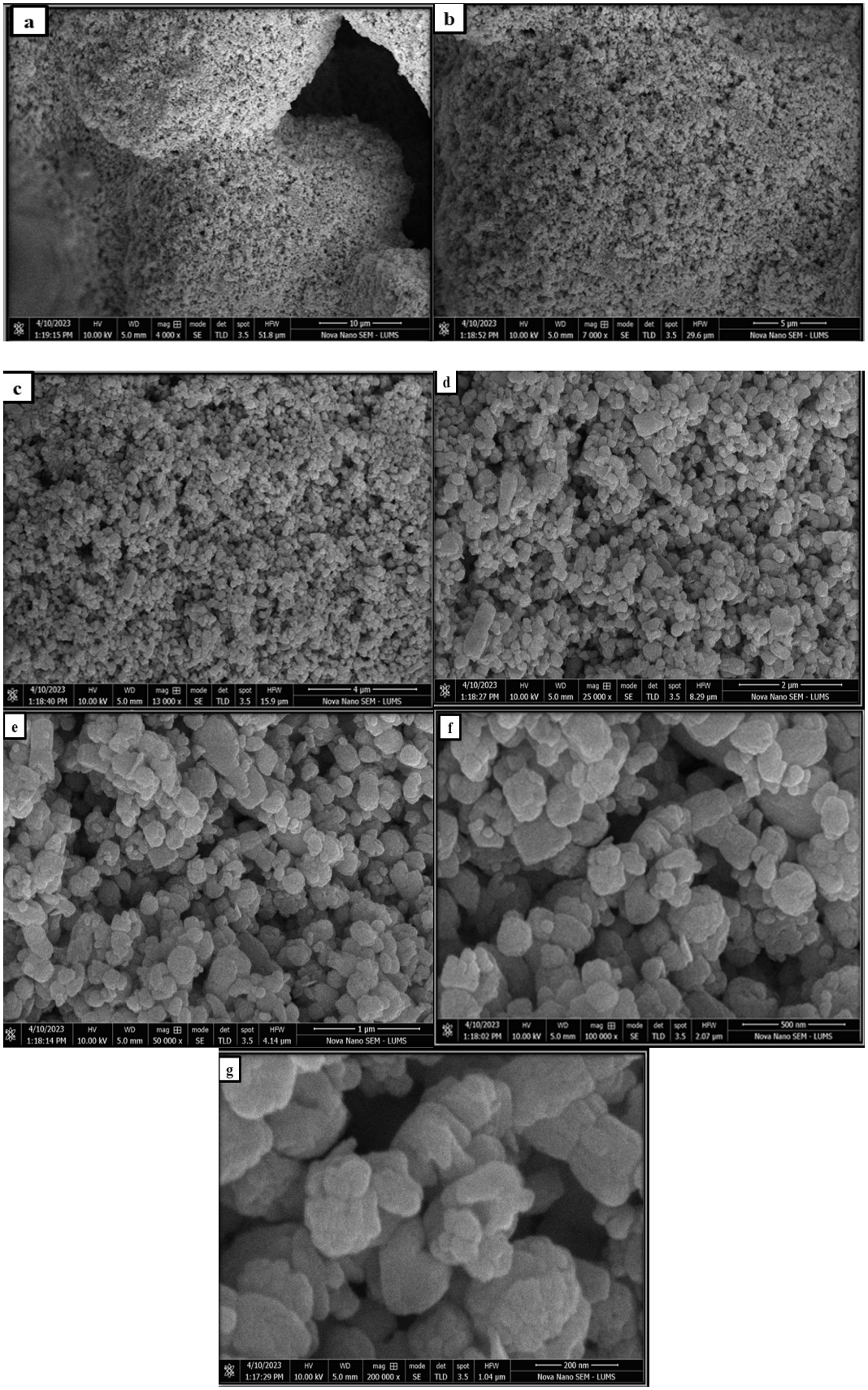

Fig. 5. (a-g) SEM images of ZnO/Ag nanohybrid at: a) 10 µm, b) 5 µm, c) 4 µm, d) 2 µm, e) 1 µm, f) 500 nm, g) 200 nm.

3.4. Antibacterial activity

The bactericidal potential from ZnO/Ag nanocomposite was identified by agar well diffusion method. Five bacterial strains used for antibacterial activity were *S. aureus*, *B. subtilis*, *E.coli*, *A. hydrophila* and *B. cereus* (Fig. 6). The results were calculated in the form of zone of inhibition (mm) at different concentrations and standards. The antibacterial potentials against strains are shown in (Fig. 7). The zones of inhibition exhibited by ZnO/Ag nanocomposite against *S. aureus* and *B. subtilis* were 15.3 ± 0.58 mm and 15.7 ± 0.58 mm respectively when ciprofloxacin was used as standard. The zones of inhibition against *E. coli*, *A. hydrophila* and *B. cereus* were 15.5 ± 0.5 mm, 11.4 ± 0.51 and 10.6 ± 0.58 respectively while gentamicin was used as a standard. The plausible mechanism was that ZnO/Ag nanohybrid got attached to the cell wall of bacterial strains. Because carboxylic acid is present in bacterial cell membranes, the surface of bacterial strains was negatively charged, but the Ag nanoparticles on the surface of ZnO were slightly electropositive. The electrostatic attraction was developed between oppositely charged species. It increased the permeability of cell membrane. ZnO/Ag nanohybrid entered the cell and deactivated enzymatic activity of bacterial respiratory chain that ultimately led to cell death. The results concluded that ZnO/Ag exhibited more antibacterial effect against *B. subtilis* than *S. aureus* because there was difference in structural and chemical composition of cell membrane of both strains. Zare et al. treated *E. coli* and *S. aureus* with ZnO/Ag nanohybrid and reported that ZnO/Ag nanohybrid had more antibacterial effect against gram positive strain *(S. aureus*) than gram negative strain (*E. coli*) [35].

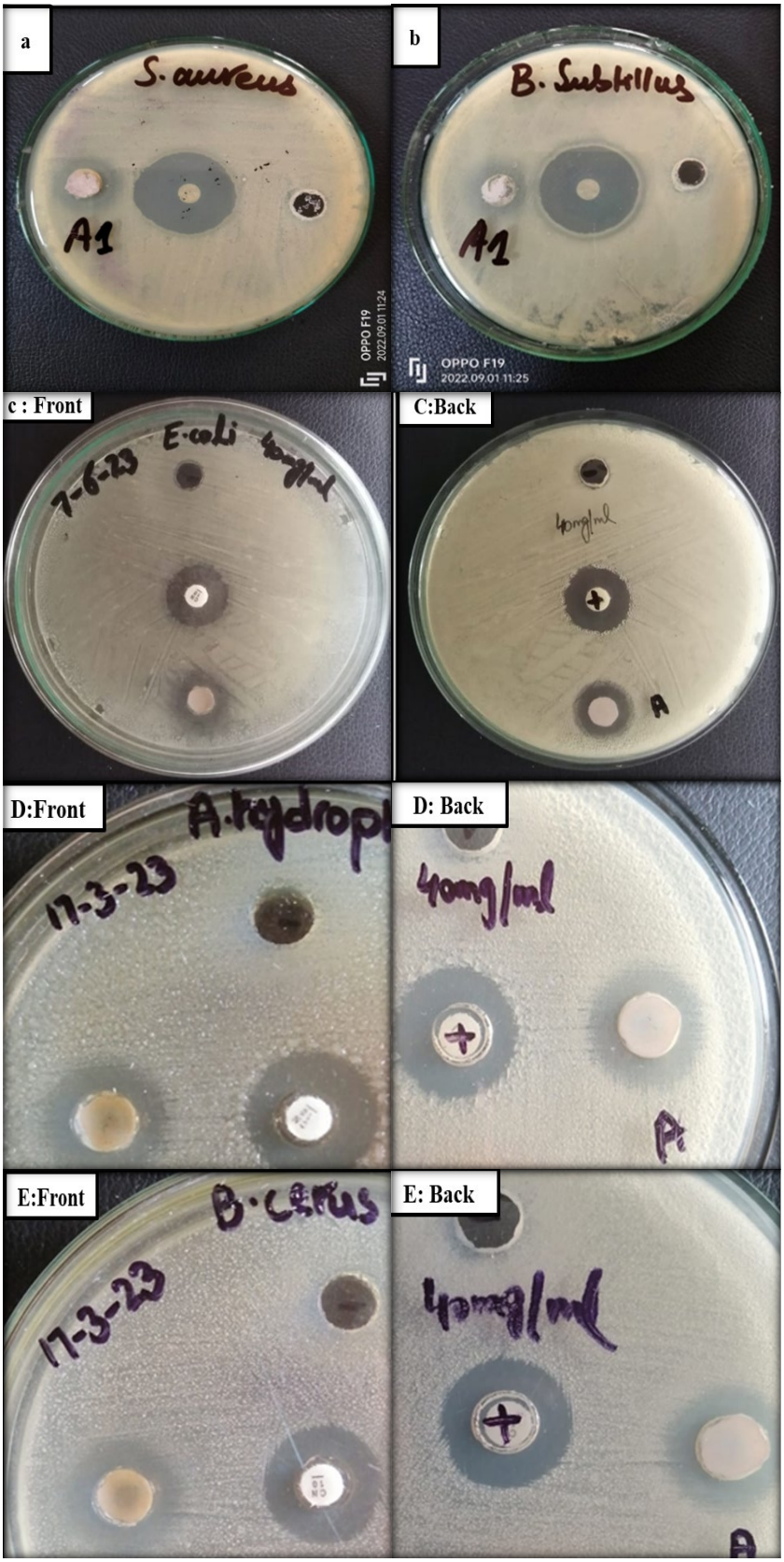

Fig. 6. (a,b) Effect of ZnO/Ag nanocomposite on growth of (a) S. aureus, (b) B. subtilis, (c) E.coli, (d) A. hydrophila, (e) B. cereus.

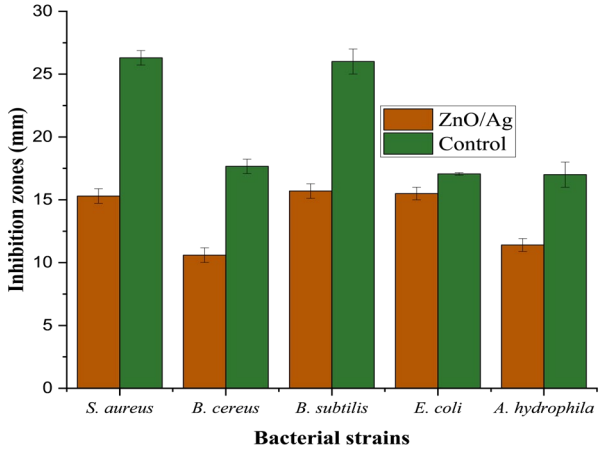

Fig. 7. Inhibition zones of ZnO/Ag nanocomposite, Ciprofloxacin and Gentamicin used as control

4. Conclusion

ZnO/Ag nanocomposite was successfully synthesized through an inexpensive route utilizing DPM as capping agent and avoiding any expensive or toxic chemicals. The green method of synthesis was biocompatible, cost effective and eco-friendly. The synthesized ZnO/Ag nanohybrid was turned to be potentially stable with zeta potential of 7.57 mV by DLS. The particles were monodispersed in a consistent manner and SEM confirmed sphere like structure of Ag particles on ZnO. The characteristics peaks of XRD confirmed ZnO's hexagon-like wurtzite structure and Ag's face-centered cubic structure. The development of nanohybrid resulted in unique physical and chemical properties. Finally, the synthesized ZnO/Ag nanohybrid was found to be antibacterial agent to kill bacteria. In the future, it may be utilized to make antibacterial cotton bandages and wound healing scaffolds.

Acknowledgements

The authors thank Ongoing Researchers Support program, (ORF-2025-1072), King Saud University, Riyadh, Saudi Arabia for financial support. The funding organization did not influence the study's design, data collection, analysis, interpretation, or publication. We sincerely appreciate lab staff that have facilitated us.

References

[1] X. Yang, W. Zhang, X. Qin, M. Cui, Y. Guo, T. Wang, K. Wang, Z. Shi, C. Zhang, W. Li, Biomimetics, 7(3), 88 (2022); https://doi.org/10.3390/biomimetics7030088

[2] J. Silvestre, N. Silvestre, J. De Brito, European Journal of Environmental and Civil Engineering, 20(4), 455 (2016); https://doi.org/10.1080/19648189.2015.1042070

[3] S.H. Khan, B. Pathak, M. Fulekar, Advanced Composites and Hybrid Materials, 3, 551 (2020); https://doi.org/10.1007/s42114-020-00174-0

[4] P.G. Jamkhande, N.W. Ghule, A.H. Bamer, M.G. Kalaskar, Journal of drug delivery science and technology, 53, 101174 (2019); https://doi.org/10.1016/j.jddst.2019.101174

[5] S. Akhtar, K. Shahzad, S. Mushtaq, I. Ali, M.H. Rafe, S.M. Fazal-ul-Karim, Materials Research Express, 6(10), 105409 (2019); https://doi.org/10.1088/2053-1591/ab3b27

[6] J.F. Banfield, H. Zhang, Reviews in mineralogy and geochemistry, 44(1), 1 (2001); https://doi.org/10.2138/rmg.2001.44.01

[7] A. Kishore, C. Singh, G. Kaur, Bio-Nanomaterials in Environmental Remediation: Industrial Applications, Wiley-VCH, Germany, 1 2025; https://doi.org/10.1002/9783527848546.ch1

[8] K. Shahzad, S. Mushtaq, M. Rizwan, W. Khalid, M. Atif, F.U. Din, N. Ahmad, R. Abbasi, Z. Ali, Materials Science and Engineering: C, 119, 111444 (2021); https://doi.org/10.1016/j.msec.2020.111444

[9] S. Mushtaq, K. Shahzad, T. Saeed, A. Ul-Hamid, B.H. Abbasi, N. Ahmad, W. Khalid, M. Atif, Z. Ali, R. Abbasi, Beilstein journal of nanotechnology, 12(1), 1339 (2021); https://doi.org/10.3762/bjnano.12.99

[10] K. Shahzad, M.A. Abbasi, M.H. Rafe, A. Pestereva, F. Ullah, M. Zaman, M. Irfan, M. Afzal, A. Orlova, Biomedical Materials, 20(1), 015021 (2024); https://doi.org/10.1088/1748-605X/ad971e

[11] M.T. Aminzai, A. Patan, Journal of Nanomaterials, 2024(1), 3280349 (2024); https://doi.org/10.1155/2024/3280349

[12] J. Nandhini, E. Karthikeyan, E.E. Rani, V. Karthikha, D.S. Sanjana, H. Jeevitha, S. Rajeshkumar, V. Venugopal, A. Priyadharshan, Engineered Regeneration, 5(3), 306 (2024); https://doi.org/10.1016/j.engreg.2024.06.004

[13] A. Al-Subaiyel, A.A. Abdellatif, Drug Development and Industrial Pharmacy, 1 (2024).

[14] J.R. Morones-Ramirez, J.A. Winkler, C.S. Spina, J.J. Collins, Science translational medicine, 5(190), 190ra81 (2013); https://doi.org/10.1126/scitranslmed.3006276

[15] E. Sulastri, R. Lesmana, M.S. Zubair, A.F.A. Mohammed, K.M. Elamin, N. Wathoni, Heliyon, 9(7), e18044 (2023); https://doi.org/10.1016/j.heliyon.2023.e18044

[16] Q. Zhou, W. Liu, Y. Long, C. Sun, G. Jiang, Silver Nanoparticles in the Environment, Springer, Berlin, 109 2015; https://doi.org/10.1007/978-3-662-46070-2_5

[17] P. Rani, V. Arya, Engineering Interventions in Agricultural Processing, Apple Academic Press, New York, 131 2017; https://doi.org/10.1201/9781315207377-6

[18] M. Cui, S. Li, X. Ma, J. Wang, X. Wang, N.E. Stott, J. Chen, J. Zhu, International Journal of Biological Macromolecules, 256, 128088 (2024); https://doi.org/10.1016/j.ijbiomac.2023.128088

[19] L. Xu, Y.-Y. Wang, J. Huang, C.-Y. Chen, Z.-X. Wang, H. Xie, Theranostics, 10(20), 8996 (2020); https://doi.org/10.7150/thno.45413

[20] R. Verma, A. Basheer Khan, Chemical Engineering & Technology, 44(5), 819 (2021); https://doi.org/10.1002/ceat.202000456

[21] T.U.D. Thi, T.T. Nguyen, Y.D. Thi, K.H.T. Thi, B.T. Phan, K.N. Pham, RSC advances, 10(40), 23899 (2020); https://doi.org/10.1039/D0RA04926C

[22] J.G. Cuadra, L. Scalschi, B. Vicedo, M. Guc, V. Izquierdo-Roca, S. Porcar, D. Fraga, J.B. Carda, Applied Sciences, 12(10), 5023 (2022); https://doi.org/10.3390/app12105023

[23] M. Shahid, F. Anjum, Y. Iqbal, S.G. Khan, T. Pirzada, Pakistan Journal of Agricultural Sciences, 57(2), (2020).

[24] H. Umar, D. Kavaz, N. Rizaner, International journal of nanomedicine, 87 (2019); https://doi.org/10.2147/IJN.S186888

[25] D. Thatikayala, V. Banothu, J. Kim, D.S. Shin, S. Vijayalakshmi, J. Park, Journal of Materials Science: Materials in Electronics, 31, 5324 (2020); https://doi.org/10.1007/s10854-020-03093-4

[26] A. Chauhan, R. Verma, S. Kumari, A. Sharma, P. Shandilya, X. Li, K.M. Batoo, A. Imran, S. Kulshrestha, R. Kumar, Scientific reports, 10(1), 7881 (2020); https://doi.org/10.1038/s41598-020-64419-0

[27] M. Zare, K. Namratha, K. Byrappa, Int. J. Sci. Res. Sci. Technol, 4(5), 1636 (2018).

[28] M. Shahid, H. Munir, N. Akhter, N. Akram, F. Anjum, Y. Iqbal, M. Afzal, International Journal of Biological Macromolecules, 191, 861 (2021); https://doi.org/10.1016/j.ijbiomac.2021.09.126

[29] M. Khatami, R.S. Varma, N. Zafarnia, H. Yaghoobi, M. Sarani, V.G. Kumar, Sustainable Chemistry and Pharmacy, 10, 9 (2018); https://doi.org/10.1016/j.scp.2018.08.001

[30] K. Shanmugam, R. Lakshmanan, R. Jagadeesan, M. Maghimaa, N. Hemapriya, S. Suresh, Chemical Physics Impact, 9, 100763 (2024); https://doi.org/10.1016/j.chphi.2024.100763

[31] A.Z. Pasha, S.A. Bukhari, H.A. El Enshasy, H. El Adawi, S. Al Obaid, Saudi Journal of Biological Sciences, 29(2), 774 (2022); https://doi.org/10.1016/j.sjbs.2021.10.048

[32] K. Haiouani, S. Hegazy, H. Alsaeedi, M. Bechelany, A. Barhoum, Materials, 17(17), 4340 (2024); https://doi.org/10.3390/ma17174340

[33] O.V. Kharissova, H.R. Dias, B.I. Kharisov, B.O. Pérez, V.M.J. Pérez, Trends in biotechnology, 31(4), 240 (2013); https://doi.org/10.1016/j.tibtech.2013.01.003

[34] K. Rajangam, K.S. Gowri, R.P. Kumar, L. Surriya, S.V. Raj, B. Balraj, S. Thangavel, Materials Research Express, 6(9), 095524 (2019); https://doi.org/10.1088/2053-1591/ab3334

[35] M. Zare, K. Namratha, S. Alghamdi, Y.H.E. Mohammad, A. Hezam, M. Zare, Q.A. Drmosh, K. Byrappa, B.N. Chandrashekar, S. Ramakrishna, Scientific reports, 9(1), 8303 (2019); https://doi.org/10.1038/s41598-019-44309-w